CATCHR and HOPS-CORVET tethering complexes share a similar architecture

HHS Public Access

Author manuscript

Nat Struct Mol Biol. Author manuscript; available in PMC 2017 January 18.

Published in final edited form as:

Nat Struct Mol Biol. 2016 August ; 23(8): 761–763. doi:10.1038/nsmb.3264.

CATCHR and HOPS-CORVET tethering complexes share a similar architecture

Hui-Ting Chou[1], **Danijela Dukovski**[1,^], **Melissa G. Chambers**[1], **Karin M. Reinisch**[2], and **Thomas Walz**[1,&,*]

[1]Department of Cell Biology, Harvard Medical School, Boston, Massachusetts, USA

[2]Department of Cell Biology, Yale University School of Medicine, New Haven, Connecticut, USA

Abstract

We show that the *Saccharomyces cerevisiae* GARP complex and the Cog1-4 subcomplex of the COG complex, both members of the complexes associated with tethering containing helical rods (CATCHR) family of multisubunit tethering complexes, share the same subunit organization. We also show that the HOPS complex, a tethering complex acting in the endolysosomal pathway, shares a similar architecture, suggesting that multisubunit tethering complexes use related structural frameworks.

Transport vesicles bring protein and lipid cargo to and from organelles. Recognition of the target membrane involves a number of proteins, including vesicle coat proteins, SNARE proteins, Rab GTPases, Sec1-Munc18 (SM) proteins, and tethering factors. Multisubunit tethering complexes (MTCs) range in size from 250 kDa to 1 MDa, are recruited to organelle membranes by Rab GTPases, and are thought to orchestrate the events that lead from vesicle recognition to membrane fusion.

MTCs are categorized into three groups: (1) MTCs that act along the secretory pathway (the CATCHR family): the Dsl1 complex, the Golgi-associated retrograde protein (GARP) complex, the endosome-associated retrograde protein (EARP) complex, the conserved oligomeric Golgi (COG) complex and the exocyst complex. These complexes are characterized by long flexible legs[1]. (2) MTCs that act in the endolysosomal pathway: the homotypic fusion and vacuole protein sorting (HOPS) complex and the class C core vacuole-endosome tethering (CORVET) complex[2]. (3) The transport protein particle (TRAPP) family: the TRAPPI, II, and III complexes. While TRAPP complexes have historically been enumerated among the MTCs, their primary role is guanine nucleotide

*Correspondence: T. W., twalz@rockefeller.edu.

^Current address: Proteostasis Therapeutics, Cambridge, Massachusetts, USA

&Current address: The Rockefeller University, New York, New York, USA

Competing Financial Interests: The authors declare no competing financial interests.

Author Contributions: T.W. and H.T.C. designed the experiments and analyzed the data. H.T.C. performed all the experiments. D.D. assisted with preparing GFP-labeled yeast strains and M.C. assisted with EM imaging and data processing. T.W., K.M.R., and H.T.C. wrote the manuscript.

exchange for the Rab GTPase Ypt1p-Rab1[3]. They appear to be functionally distinct from the other two MTC groups as they have no reported role in SNARE recruitment or assembly. As discussed below, the TRAPP complexes also have a different, more compact architecture from that of other MTCs.

We set out to characterize the structure of the yeast GARP and HOPS complexes. We first used tandem affinity purification (TAP) to isolate the GARP complex (Supplementary Fig. 1a and Supplementary Table 1). Negative-stain EM images showed Y-shaped complexes (Supplementary Fig. 1b), and class averages revealed substantial structural variability (Supplementary Fig. 1c). The three legs, labeled A to C in Figure 1a, can be distinguished by leg A being the shortest one, leg B ending in a compact “hook” density (arrowheads in Fig. 1a), and leg C featuring a hinge in the middle (arrows in Fig. 1a).

To establish the subunit organization of the GARP complex we used a GFP-tagging approach. We first expressed GARP complex with a C-terminal GFP on Vps51 (Supplementary Fig. 1d) and imaged the complex by negative-stain EM (Supplementary Fig. 1e). Some class averages showed extra density for the GFP and located the Vps51 C terminus to the hinge region of leg C (Fig. 1b). Most averages, however, were poorly defined (Supplementary Fig. 1f), making it difficult to unambiguously identify the location of the GFP. We therefore decided to change to a double-GFP-tagging strategy and to analyze raw particle images.

The results of double-GFP tagging (Fig. 1c-i, Supplementary Note 1 and Supplementary Figs. 2 and 3a-g) and of a Vps51 deletion (Supplementary Fig. 3h) allowed us to establish how the subunits are arranged in the GARP complex (Fig. 1j). Leg A is formed by the C-terminal region of Vps52, and the distal segments of legs B and C are formed by the C-terminal regions of Vps53 and Vps54, respectively. The N-terminal region of Vps54 also contributes to the proximal region of leg B. All of Vps51 and the N-terminal regions of the other three subunits form the proximal segment, up to the hinge, of leg C.

The subunit organization of the GARP complex is very similar to that of the Cog1-4 subcomplex[4] (Fig. 1k). Even though the corresponding subunits have very low sequence similarity, comparison of the projection structures shows that structurally Vps51 corresponds to Cog2, Vps52 to Cog3, Vps53 to Cog4, and Vps54 to Cog1. The similarity between the corresponding subunits is also reflected in the crystal structures of the C termini of GARP subunit Vps53[5] and the corresponding subunit, Cog4, of the Cog1-4 subcomplex[6] (Supplementary Fig. 4a,b). Note that subunits Vps51 and Cog2 are longer in humans[7,8] than in yeast (Fig. 1j,k). The N-terminal regions of the GARP subunits have been implicated in SNARE binding[9], but so far only Cog4 was found to interact with SNAREs[10], so that it is currently unclear whether the Cog1-4 subcomplex interacts with SNAREs in the same way as the GARP complex.

We also purified yeast HOPS complex containing all six subunits (Supplementary Fig. 4c, Supplementary Table 2). Negative-stain EM images revealed particles with flexible rod-like extensions (Supplementary Fig. 4d), markedly different from the more globular and rigid particles reported before[11]. The previous study used chemical cross-linking to stabilize the

complex, and when we exposed our HOPS preparation to glutaraldehyde we found that the particles became more similar in shape to those reported earlier (Supplementary Fig. 4e).

Class averages revealed that the HOPS complex is not only very flexible but also easily falls apart (Supplementary Fig. 5a). The largest particles show that the HOPS complex consists of a head and extended legs (Fig. 2a, averages 1-4). The head comprises two domains (marked as I and II in Fig. 2a, average 1): a larger bipartite domain and a smaller globular domain that is lacking in some complexes (Fig. 2a, averages 5 and 6). The head is attached to a long, filamentous structure with a diffuse density near its center. In some class averages, this diffuse density appears like a strongly bent leg (arrow in Fig. 2a, average 2). We thus interpret the filamentous structure to represent three legs (labeled A to C in Fig. 2a, average 1). This assignment is supported by class averages of complexes that lack leg A (Fig. 2a, averages 7 and 8) or leg C (Fig. 2a, averages 9 and 10).

Comparison of our projection structure with available literature[11,12] allowed us to deduce the likely subunit organization of HOPS (Fig. 2b, Supplementary Note 2 and Supplementary Fig. 5b-h). Comparison with the GARP complex (Fig. 2c) suggests that HOPS subunits Vps11, Vps18, Vps39 and Vps41 are analogous to GARP subunits Vps51 to Vps54. While HOPS Vps11 would correspond to GARP Vps51, the correspondence between the other three subunits is ambiguous. Nevertheless, all HOPS subunits except Vps33 consist of N-terminal β-propellers and C-terminal α-solenoids and likely interact through their C termini[13], so that they may interact with each other in the same way as the N termini of GARP subunits, i.e., through the formation of helical bundles. HOPS subunits Vps16 and Vps33 would be unique to the HOPS complex. As Vps33 has the fold of an SM protein[13,14], it may be that the HOPS and CORVET complexes evolved to have a “built-in” SM protein, whereas CATCHR complexes associate less stably, maybe very transiently, with SM proteins[15].

In summary, we find first that the CATCHR assemblies GARP and Cog1-4[4] are structurally very similar at low resolution, and as EARP is identical to GARP in composition, other than that syndetin replaces Vps54 (Fig. 2c), it likely also has the same organization. A recent negative-stain EM study of the hetero-octameric exocyst complex[16] suggests it is similarly multi-legged, although the legs appear to interact more extensively than in the COG[17] and GARP complexes. Dsl, the smallest and most divergent of the CATCHR complexes, is multi-legged, but the three subunits interact differently[18]. Furthermore, our data suggest that HOPS is similarly multi-legged as the CATCHR complexes and that its subunits may interact as in the GARP and Cog1-4 complexes. The HOPS and CORVET complexes share four of their six subunits, and so will be organized in the same way. Thus, it appears that the tethering complexes of the secretory and endolysosomal pathways share a common building plan, reflecting their analogous functions.

Online Methods

Yeast strains and plasmids

The yeast strains used in this work are summarized in Supplementary Table 3. GARP complexes with and without GFP tags were purified using strains with a C-terminal TAP tag

on Vps54 or Vps52. The strain expressing TAP-tagged Vps54 was purchased from the Open Biosystems Collection (background strain BY4741). The strain expressing TAP-tagged Vps52 was generated by using homologous recombination to add the sequence for TAP::HIS3MX6 to the 3′ end of the Vps52 gene.

The strains used to express GARP subunits with a C-terminal GFP tag were prepared by adding the sequence for GFP::KanMX6 or GFP::hphNT1 to the 3′ end of the genes encoding the subunits. To make strains expressing GARP subunits with N-terminal GFP tags, a DNA fragment containing the first 800 bp upstream of Vps52, the GFP sequence and 300 bp downstream of Vps52 was ligated into the pRS416 vector using the KpnI-XhoI, XhoI-HindIII and XbaI-NotI restriction sites. Then, one of the genes encoding Vps51, Vps52, Vps53 or Vps54 was added to the 3′ end of the GFP sequence using the SmaI-BamHI or SmaI-SpeI restriction sites. These constructs were used to transform yeast strains in which the genes for the respective subunits were deleted.

The HOPS complex was purified using a strain with a C-terminal TAP tag on Vps41, which was purchased from the Open Biosystems Collection (background strain BY4741).

Purification of the GARP and HOPS complexes

The GARP and HOPS complexes were purified using the standard TAP purification protocol. Yeast cells were grown in 18 L YPD medium, and when OD_{600} reached 2 to 2.5, the cells were harvested by centrifugation at 4,000×g for 10 min at 4°C. The pellets were frozen, ground up by hand, and broken with a bead beater (BioSpect Products Inc.) in lysis buffer (6 mM Na_2HPO_4, 4 mM NaH_2PO_4, pH 7.2, 150 mM NaCl, 2 mM EDTA, 1 mM EGTA, 0.1 mM Na_3VO_4, 0.1% NP-40 and 50 mM NaF). The lysate was cleared by centrifugation at 20,000×g for 40 min at 4°C, and the supernatant was incubated with IgG Sepharose resin (GE HealthCare) for 1 hour at 4°C. The resin was washed with buffer A (10 mM Tris-HCl, pH 8.0, 150 mM NaCl, and 0.1% NP-40) and incubated with TEV protease for 1.5 h at 16°C. The suspension was loaded into a column, and the flow-through was incubated with Calmodulin Sepharose resin (GE HealthCare). After loading the resin into a column, it was washed first with 0.1% and then with 0.01% NP-40 in CBB buffer (10 mM Tris-HCl, pH 8.0, 150 mM NaCl, 1 mM magnesium acetate, 1 mM imidazole, 2 mM $CaCl_2$, and 1 mM DTT). GARP or HOPS complex was eluted with elution buffer (CBB buffer with 0.01% NP-40, but containing 20 mM EGTA instead of 2 mM $CaCl_2$) and used immediately for negative-stain EM.

For analysis by tandem mass spectrometry, Vps54 TAP-tagged GARP complex eluting from the Calmodulin Sepharose column was precipitated with trichloroacetic acid (TCA) and analyzed (Supplementary Table 1). In the case of Vps41 TAP-tagged HOPS complex, protein eluting from the Calmodulin Sepharose column was run on an SDS-PAGE gel, and the region of the gel marked by a bracket in Supplementary Fig. 4c was cut out and analyzed (Supplementary Table 2).

For cross-linking, HOPS complex was incubated with 0.008% (v/v; final concentration) glutaraldehyde (EM grade, Electron Microscopy Sciences) for 10 min on ice. The cross-

linking reaction was stopped by adding 1 M Tris-HCl, pH 8.0, to a final concentration of 80 mM.

Electron microscopy

Samples were negatively stained with 0.75% (w/v) uranyl formate and imaged with an FEI Tecnai 12 electron microscope operated at an acceleration voltage of 120 kV using low-dose procedures. HOPS complex, untagged GARP complex and GARP complex with a C-terminal GFP on Vps51 were imaged at a nominal magnification of 67,000× with a defocus of –1.5 μm. The images were taken on image plates, which were digitized with a DITABIS scanner (DITABIS Digital Biomedical Imaging System AG, Pforzheim, Germany) using a step size of 15 μm. The images were binned over 2 × 2 pixels, resulting in a pixel size of 4.48 Å on the specimen level.

Images of double-GFP-tagged GARP complexes were recorded on a Gatan 4K × 4K CCD camera with an underfocus range of 2.5 - 3.0 μm. The nominal magnification was 67,000× and the calibrated pixel size was 1.68 Å on the specimen level. The images were binned over 2 × 2 pixels, resulting in a pixel size of 3.36 Å. Cross-linked HOPS was imaged with a Gatan 4K × 4K CCD camera at a nominal magnification of 42,000×, resulting in a calibrated pixel size of 2.61 Å on the specimen level.

Image processing

For untagged GARP complex, 15,369 particles were picked and windowed into 110 × 110-pixel images. After normalization and reducing the particle images to 64 × 64 pixels, the particles were aligned and classified using the Interactive Stable Alignment and Clustering (ISAC) procedure[19] implemented in SPARX[20], specifying 100 particles per group and a pixel error threshold of 2. After 14 generations of ISAC, 5,737 particles (37.3% of the data set) were classified into 231 classes. For GARP complex tagged with a C-terminal GFP on Vps51, 5,355 particles were manually picked, windowed and classified into 50 classes using the *K*-means algorithm implemented in SPIDER.

For the HOPS complex, 20,714 particles were picked and windowed into 150 × 150-pixel images. After normalization and reducing the particle images to 64 × 64 pixels, the particles were subjected to ISAC, specifying 50 particles per group and a pixel error threshold of 2. After 11 generations, 3,580 particles (17.3% of the data set) were classified into 238 classes. The particles were also classified into 200 classes using *K*-means classification in SPIDER. Particles in classes giving poor averages and in classes containing subcomplexes were discarded, and the remaining 9,300 particles were classified again using *K*-means classification, specifying 50 classes.

Supplementary Material

Refer to Web version on PubMed Central for supplementary material.

Acknowledgments

We thank D. Finley and S. Elsasser (Harvard Medical School, Boston, Massachusetts, USA) for providing vectors and advice on generating the yeast strains used for N-terminal GFP tagging. This work was supported by NIH grant P01 GM062580 (to T.W.). K.R. is supported by GM80616.

References

1. Yu IM, Hughson FM. Annu Rev Cell Dev Biol. 2010; 26:137–156. [PubMed: 19575650]
2. Solinger JA, Spang A. FEBS J. 2013; 280:2743–2757. [PubMed: 23351085]
3. Yu S, Liang Y. Cell Mol Life Sci. 2012; 69:3933–3944. [PubMed: 22669257]
4. Lees JA, Yip CK, Walz T, Hughson FM. Nat Struct Mol Biol. 2010; 17:1292–1297. [PubMed: 20972446]
5. Vasan N, Hutagalung A, Novick P, Reinisch KM. Proc Natl Acad Sci USA. 2010; 107:14176–14181. [PubMed: 20660722]
6. Richardson BC, et al. Proc Natl Acad Sci USA. 2009; 106:13329–13334. [PubMed: 19651599]
7. Pérez-Victoria FJ, et al. Mol Biol Cell. 2010; 21:3386–3395. [PubMed: 20685960]
8. Ungar D, et al. J Cell Biol. 2002; 157:405–415. [PubMed: 11980916]
9. Pérez-Victoria FJ, Bonifacino JS. Mol Cell Biol. 2009; 29:5251–5263. [PubMed: 19620288]
10. Laufman O, Hong W, Lev S. J Cell Sci. 2013; 126:1506–1516. [PubMed: 23378023]
11. Bröcker C, et al. Proc Natl Acad Sci USA. 2012; 109:1991–1996. [PubMed: 22308417]
12. Ostrowicz CW, et al. Traffic. 2010; 11:1334–1346. [PubMed: 20604902]
13. Graham SC, et al. Proc Natl Acad Sci USA. 2013; 110:13345–13350. [PubMed: 23901104]
14. Baker RW, Jeffrey PD, Hughson FM. PLoS ONE. 2013; 8:e67409. [PubMed: 23840694]
15. Laufman O, Kedan A, Hong W, Lev S. EMBO J. 2009; 28:2006–2017. [PubMed: 19536132]
16. Heider MR, et al. Nat Struct Mol Biol. 2016; 23:59–66. [PubMed: 26656853]
17. Ha JY, et al. Nat Struct Mol Biol. 2016 This issue.
18. Ren Y, et al. Cell. 2009; 139:1119–1129. [PubMed: 20005805]
19. Yang Z, Fang J, Chittuluru J, Asturias FJ, Penczek PA. Structure. 2012; 20:237–247. [PubMed: 22325773]
20. Hohn M, et al. J Struct Biol. 2007; 157:47–55. [PubMed: 16931051]

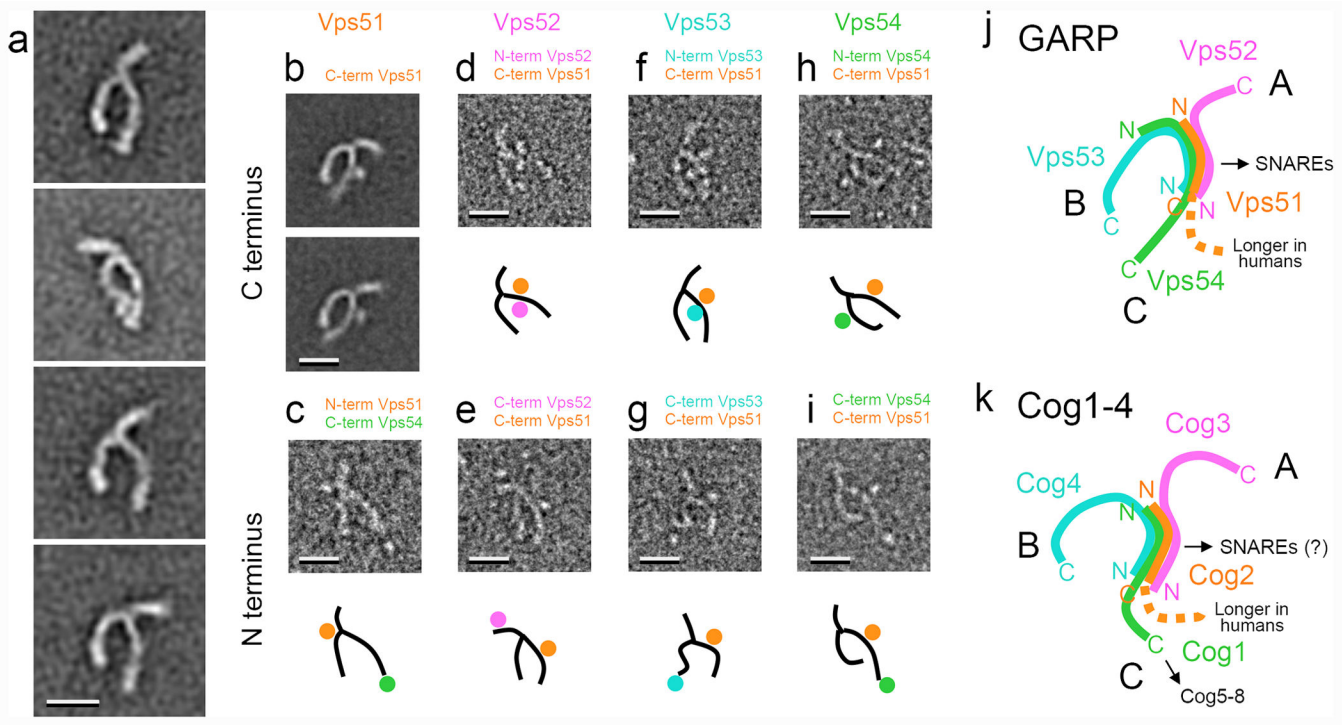

Figure 1.

Subunit organization of the yeast GARP complex and comparison with the Cog1-4 subcomplex. (**a**) Selected averages of the GARP complex. The three legs of the Y-shaped complex are labeled from the shortest leg (A) to the longest leg (C). The arrowheads point to a hook at the end of leg B and the arrows point to a hinge in the middle of leg C. (**b**) Selected class averages of GARP complex tagged with GFP at the C terminus of Vps51 (see Supplementary Fig. 1f for all class averages). The GFP (indicated by arrows) is located close to the hinge region in leg C. (**c**) Raw particle image (top panel) and schematic drawing (bottom panel) of GARP complex with an N-terminal GFP on Vps51. A C-terminal GFP on Vps54 was used to mark leg C. See Supplementary Fig. 3g for additional particles. **(d - i)** Raw particle images (top panels) and schematic drawings (bottom panels) of GARP complexes with a GFP at the N terminus (d) or C terminus (e) of Vps52, at the N terminus (f) or C terminus (g) of Vps53, and at the N terminus (h) or C terminus (i) of Vps54. A C-terminal GFP on Vps51 was used to mark leg C. See Supplementary Fig. 3a-f for additional particles. Scale bars in panels (a) to (i) are 15 nm. (**j**, **k**) Schematic drawings of the GARP complex (j) and the Cog1-4 subcomplex (k), revealing which subunits in the two complexes correspond to each other.

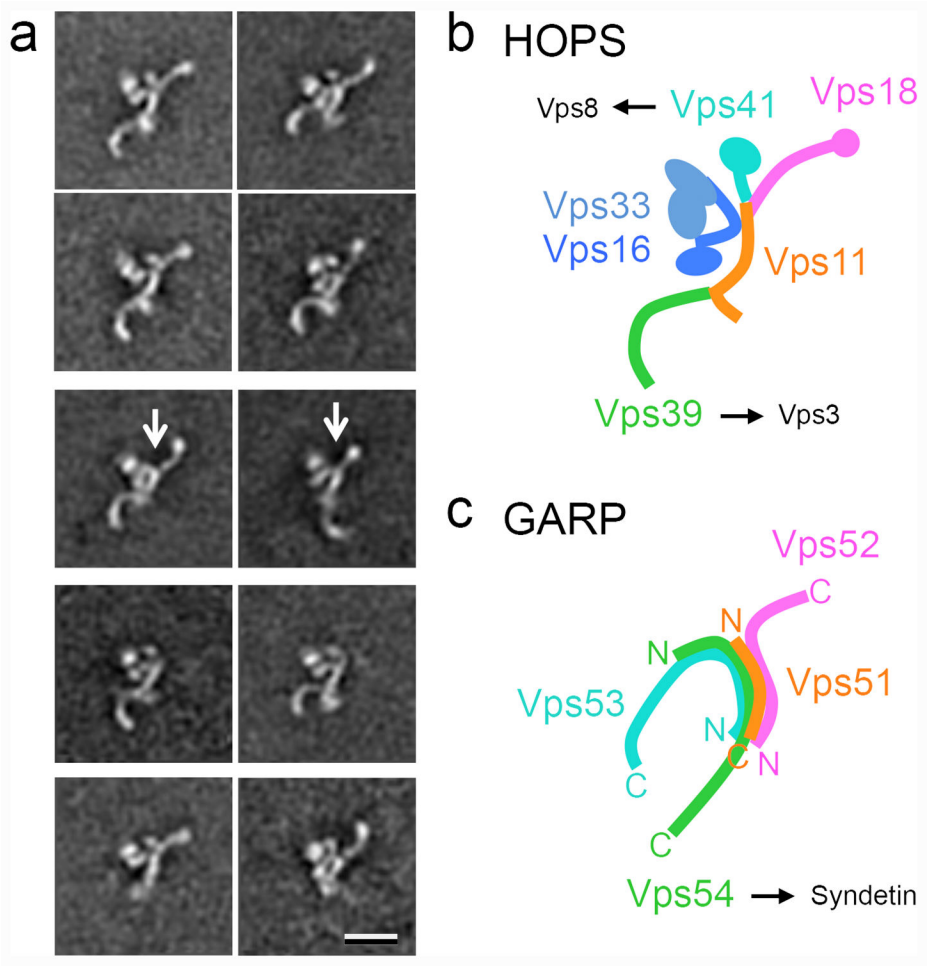

Figure 2.

Proposed subunit organization of the HOPS complex and comparison with the GARP complex. (**a**) Selected averages of the full HOPS complex and different subcomplexes. Averages 1 to 4 illustrate the structural variability of the HOPS complex. In average 1 the structural features of the HOPS complex are marked. The arrow in average 2 points to leg B that usually appears as a smeared-out density. Averages 5 and 6 show subcomplexes missing domain II. Averages 7 and 8 show subcomplexes missing leg A. Averages 9 and 10 show subcomplexes missing leg C. The arrows in panels 5 to 10 point to the area where the missing domains would be located in the full complex. The scale bar is 20 nm. (**b**, **c**) Schematic drawings of the HOPS complex (b) and the GARP complex (c), revealing which subunits in the two complexes potentially correspond to each other. Arrows and protein names indicate the protein substitutions that convert the HOPS to the CORVET complex and the GARP to the EARP complex.